

## Communications

Facile Synthesis of Graphene-supported MnO, Mn<sub>3</sub>O<sub>4</sub>, and MnO<sub>2</sub> Nanocomposites by Controlling Gas EnvironmentSeokhoon Ahn, Sang Myeong Kang,<sup>†</sup> Soul-Hee Lee,<sup>†</sup> and Joon B. Park<sup>†,‡,\*</sup><sup>†</sup>Institute of Advanced Composite Materials, Korea Institute of Science and Technology, Jeonbuk 565-950, Korea<sup>‡</sup>Department of Chemistry Education and Institute of Fusion Science, Chonbuk National University, Jeonju 561-756, Korea

\*E-mail: joonbumpark@jbnu.ac.kr

<sup>‡</sup>Department of Bioactive Material Sciences and Research Center of Bioactive Materials, Chonbuk National University, Jeonju 561-756, Korea

Received July 3, 2014, Accepted July 11, 2014

**Key Words :** Graphene, Manganese oxide, XRD, TEM, XPS

Graphene is one of the most fascinating materials today due to its extraordinary electronic, mechanical, and thermal properties as well as its extremely high specific surface area.<sup>1-3</sup>

These unique properties offer great potential as two-dimensional supports to host nanomaterials. MnO<sub>x</sub> nanocomposites have attracted increasing attention in photocatalysis, energy storage, and Li ion batteries because of their low cost, environmental abundance, and high theoretical specific capacitances.<sup>4,5</sup> Recently, several research groups have reported that graphene-supported MnO<sub>x</sub> nanocomposites can play a critical role in energy storage<sup>5-7</sup> and can be prepared by using an aqueous chemical method,<sup>8</sup> chemical reduction,<sup>9-11</sup> and colloidal mixing.<sup>12</sup> However, these methods are somewhat complicated and require different synthetic protocols to prepare specific MnO<sub>x</sub> nanoparticles (NPs) on graphene, which makes it difficult to produce those nanocomposites. In this study, we have developed a straightforward synthetic route to synthesize specific MnO<sub>x</sub>/G nanocomposites by controlling gas environment. The method involves preparation of graphite oxide (GO) from graphite, impregnation of Mn<sup>2+</sup> precursor on GO (Mn<sup>2+</sup>/GO), and thermal treatment in H<sub>2</sub>, Ar, and air environment to produce MnO/G, Mn<sub>3</sub>O<sub>4</sub>/G, and MnO<sub>2</sub>/G, respectively.

GO was prepared by exfoliation and oxidation of graphite powder according to the modified Hummers and Offeman's method.<sup>4</sup> For the synthesis of MnO/G and Mn<sub>3</sub>O<sub>4</sub>/G, GO (0.2 g) was mixed with Mn(CH<sub>3</sub>COO)<sub>2</sub>·4H<sub>2</sub>O (0.89 g) in 200 mL of distilled water. Hydrazine monohydrate (5 mL, 80%) was added to the mixture and stirred for 24 h to promote the intercalation of Mn<sup>2+</sup> on the GO. The suspension was filtered and washed with distilled water several times. The filtrate was dried at 60 °C for 24 h to remove water. Thermal heating was carried out using a home-built gas flow reactor described elsewhere.<sup>4</sup> H<sub>2</sub> gas (100 sccm) and Ar gas (100 sccm) were introduced to the reactor for 5 h at 500 °C to

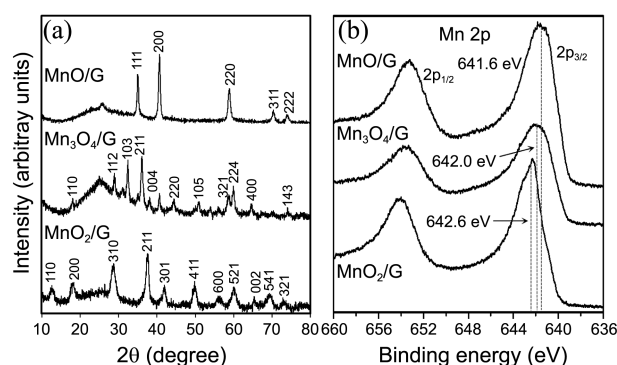


**Figure 1.** (a) XRD patterns and (b) XPS data of MnO/G, Mn<sub>3</sub>O<sub>4</sub>/G, and MnO<sub>2</sub>/G.

obtain MnO/G and Mn<sub>3</sub>O<sub>4</sub>/G, respectively. For the synthesis of MnO<sub>2</sub>/G, MnCl<sub>2</sub>·4H<sub>2</sub>O (0.81 g) was dispersed with GO in isopropyl alcohol (150 mL) under continuous ultrasonication and the mixture was heated to 83 °C. KMnO<sub>4</sub> (0.45 g) was added and stirred for 30 min. The obtained mixture was filtered, and washed with ethanol and distilled water several times. The thermal heating of the filtrate in air at 300 °C for 1 h generated the MnO<sub>2</sub>/G. TEM measurements were performed using a Tecnai G2 F20 (FEI Co.). Powder XRD analyses were performed on a multi-purpose high performance X-ray diffractometer (PANalytical). XPS spectra were acquired using Mg K<sub>α</sub> (hν = 1253.6 eV) radiation (KRATOS, AXIS Nova).

Figure 1(a) shows typical XRD patterns obtained from MnO/G (H<sub>2</sub>), Mn<sub>3</sub>O<sub>4</sub>/G (Ar), and MnO<sub>2</sub>/G (air). The sharp characteristic peaks indicate that the specific manganese oxides are composed of highly crystalline nanostructures on graphene. All the diffraction peaks of MnO/G, Mn<sub>3</sub>O<sub>4</sub>/G, and MnO<sub>2</sub>/G could be readily indexed to a cubic phase of MnO [space group: *Fm-3m* (225), JCPDS 07-0230], the tetragonal hausmannite crystal structure of Mn<sub>3</sub>O<sub>4</sub> [*I41/amd* (141),

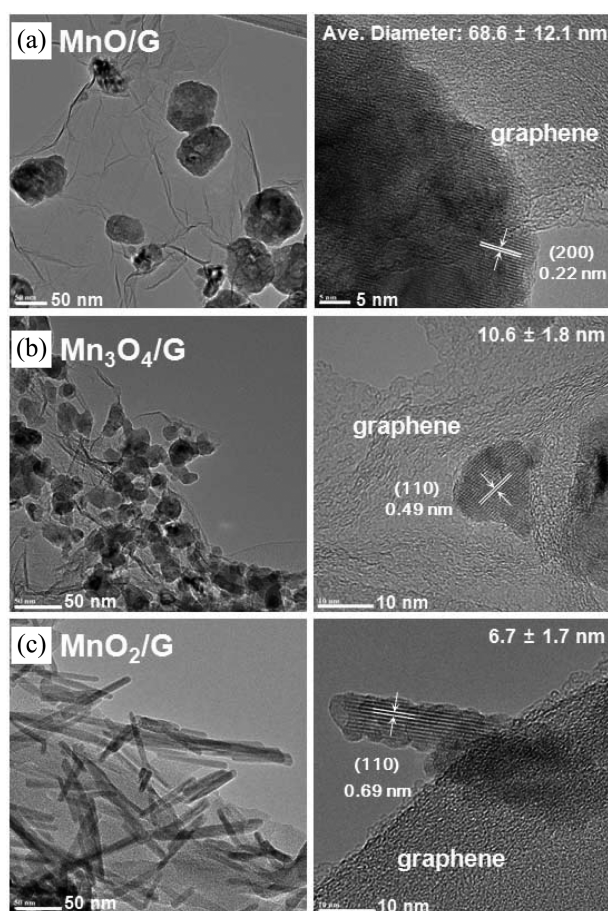


**Figure 2.** TEM images of (a) MnO/G (b) Mn<sub>3</sub>O<sub>4</sub>/G and (c) MnO<sub>2</sub>/G.

JCPDS 24-0734], and the tetragonal phase of  $\alpha$ -MnO<sub>2</sub> [I4/m (87), JCPDS 44-0141], respectively. All of the XRD patterns present a weak and broad (002) peak of the graphene at  $2\theta = 25^\circ$  with a d-spacing of 3.7 Å. This represents that oxygen and water were removed from the GO during the thermal treatments, and most of the GO was reduced into graphene.

In order to understand the effect of gas on the synthesis of MnO<sub>x</sub>/G, the oxidative structures were examined by XPS measurements. Figure 1(b) shows the Mn 2p core-level spectra of MnO/G, Mn<sub>3</sub>O<sub>4</sub>/G, and MnO<sub>2</sub>/G. The Mn atoms in MnO/G (H<sub>2</sub>) mainly consisted of +2 oxidation state, as evident from the measured binding energies of Mn 2p<sub>3/2</sub> (641.6 eV) and Mn 2p<sub>1/2</sub> (653.2 eV) peaks. In Mn<sub>3</sub>O<sub>4</sub>/G (Ar) and MnO<sub>2</sub>/G (air), the peaks shifted to higher BE by 0.4 eV and 1.0 eV, respectively. The components of Mn 2p<sub>3/2</sub> at 642.0 eV (Mn<sub>3</sub>O<sub>4</sub>/G) and Mn 2p<sub>3/2</sub> at 642.6 eV (MnO<sub>2</sub>/G) are characteristic of Mn (+2.7) and Mn (+4), respectively. All of the samples show a consistent spin-energy separation value of 11.6 eV between Mn 2p<sub>3/2</sub> and Mn 2p<sub>1/2</sub> peaks. The fact that the oxidative state of Mn in MnO<sub>x</sub>/G changes with the gas environment could explain the mechanism for the selective synthesis of a specific MnO<sub>x</sub>/G. Thus, these XPS analyses clearly proved that the gas environment plays a key role in determining MnO<sub>x</sub> structures.

The morphology and microstructures of the MnO<sub>x</sub>/G were investigated by TEM. Figure 2(a) show typical TEM images

of the MnO/G. The MnO NPs are distributed uniformly on the graphene sheets without obvious aggregation. The average diameter of the MnO NPs was measured to be  $68.6 \pm 12.1$  nm. The lattice fringes are about 0.22 nm, corresponding to the (200) facet of MnO. For the Mn<sub>3</sub>O<sub>4</sub>/G (Figure 2(b)), relatively smaller Mn<sub>3</sub>O<sub>4</sub> NPs with an average diameter of  $10.6 \pm 1.8$  nm are distributed on the wrinkled graphene sheet. Figure 2(c) shows TEM images of MnO<sub>2</sub>/G. The MnO<sub>2</sub> NPs show a needle-like morphology with an average diameter of  $6.7 \pm 1.7$  nm and length of  $72.0 \pm 31.1$  nm. It can be clearly seen that the MnO<sub>2</sub> nanoneedles decorate the terrace and edge of the graphene. These TEM results prove that a specific MnO<sub>x</sub> could be selectively prepared on graphene by controlling gas environment.

In summary, a facile synthesis of MnO/G, Mn<sub>3</sub>O<sub>4</sub>/G, and MnO<sub>2</sub>/G was developed using simple thermal reductions of Mn<sup>2+</sup>/GO in H<sub>2</sub>, Ar, and air, respectively. The analyses of XRD, XPS and TEM data clearly demonstrate the formation of crystalline MnO, Mn<sub>3</sub>O<sub>4</sub>, and MnO<sub>2</sub> NPs on graphene. Since the MnO<sub>x</sub>/G nanocomposites hold great potential for applications in catalysis, biosensors, and energy storage, this facile synthetic route of a specific MnO<sub>x</sub> on graphene offers a useful approach in various contexts from the laboratory to industrial production.

**Acknowledgments.** This research was supported by the Basic Science Research Program through NRF of Korea funded by the Ministry of Education Science and Technology (No. 2012-0003300), “Industry-University-Research Institute Core Technology Development & Industrialized Supporting Business” supported by Chonbuk Province in 2013 (2013C14), and the Korea Institute of Science and Technology Institutional Program.

## References

- Li, Y.; Fan, X. B.; Qi, J. J.; Ji, J. Y.; Wang, S. L.; Zhang, G. L.; Zhang, F. B. *Nano Res.* **2010**, 3, 429.
- Lee, K. H.; Han, S. W.; Kwon, K. Y.; Park, J. B. *J. Colloid Interf. Sci.* **2013**, 403, 127.
- Chen, S.; Zhu, J. W.; Wu, X. D.; Han, Q. F.; Wang, X. *ACS Nano* **2010**, 4, 2822.
- Chen, Z. W.; Jiao, Z.; Pan, D. Y.; Li, Z.; Wu, M. H.; Shek, C. H.; Wu, C. M. L.; Lai, J. K. L. *Chem. Rev.* **2012**, 112, 3833.
- Najafpour, M. M.; Rahimi, F.; Amini, M.; Nayeri, S.; Bagherzadeh, M. *Dalton Trans.* **2012**, 41, 11026.
- Sun, Y. M.; Hu, X. L.; Luo, W.; Xia, F. F.; Huang, Y. H. *Adv. Funct. Mater.* **2013**, 23, 2436.
- Hsieh, C. T.; Lin, C. Y.; Lin, J. Y. *Electrochim. Acta* **2011**, 56, 8861.
- Wang, H. L.; Cui, L. F.; Yang, Y. A.; Casalongue, H. S.; Robinson, J. T.; Liang, Y. Y.; Cui, Y.; Dai, H. J. *J. Am. Chem. Soc.* **2010**, 132, 13978.
- Nam, I.; Kim, N. D.; Kim, G. P.; Park, J.; Yi, J. J. *Power Sources* **2013**, 244, 56.
- Kim, M.; Hwang, Y.; Kim, J. J. *Power Sources* **2013**, 239, 225.
- Chandra, S.; Das, P.; Bag, S.; Bhar, R.; Pramanik, P. *Mater. Sci. Eng. B* **2012**, 177, 855.
- Zhang, J. T.; Jiang, J. W.; Zhao, X. S. *J. Phys. Chem. C* **2011**, 115, 6448.